ChemComm

COMMUNICATION

View Article Online
View Journal | View Issue

Cite this: *Chem. Commun.*, 2024, **60**, 4350

Received 16th February 2024,
Accepted 20th March 2024

DOI: 10.1039/d4cc00772g

rsc.li/chemcomm

Pillar[6]MaxQ functions as an *in vivo* sequestrant for rocuronium and vecuronium†

Wanping Zhang,‡[a] Emmanuel A. Bazan-Bergamino,‡[b] Anton P. Doan,[b] Xiangjun Zhang*[a] and Lyle Isaacs *[b]

The binding affinity of pillar[6]MaxQ toward a panel of neuromuscular blockers and neurotransmitters was measured in phosphate buffered saline by isothermal titration calorimetry and ^{1}H NMR spectroscopy. *In vivo* efficacy studies showed that P6MQ sequesters rocuronium and vecuronium and reverses their influence on the recovery of the train-of-four (TOF) ratio.

The development of supramolecular chemistry can be traced from early work on the fundamentals of non-covalent interactions, through the use of non-covalent interactions to build up multicomponent self-assembled systems, toward the development of supramolecular systems with application in chemistry, analytical chemistry, materials science, and medicine.[1] Macrocycles have long played a starring role in supramolecular chemistry due to their inherent preorganization which can result in high binding affinity and high selectivity in organic solvents and in water. Some of the most popular macrocyclic hosts include cyclodextrins, calixarenes, resorcinarenes and related species, cucurbituril (CB[*n*]) type receptors, cyclophanes, molecular baskets, and most recently pillararenes.[2] Macrocycles that display good water solubility and biocompatibility are well suited for a variety of biomedical applications. For example, β-cyclodextrin derivatives are used as solubilizing excipients to formulate a variety of insoluble drugs for human use.[3] The Smith group has used tetralactam macrocycles as the basis of squaraine rotaxanes for imaging applications, whereas the Kim group used cucurbituril derived supramolecular hydrogels for stem cell therapy.[4] The Guo group has used azocalixarene derivatives for numerous applications including hypoxia imaging.[5] Our group has demonstrated the use of CB[*n*]-type receptors – with their ultratight binding properties[2d] – as *in vivo* sequestrants to counteract the effects of a variety of biologically active substances.[6] Perhaps the most stunning real-world application of a macrocyclic host is the clinical use of the γ-cyclodextrin derivative sugammadex to alleviate the post-surgical side effects of the neuromuscular blocking agents (NMBA) rocuronium (roc) and vecuronium (vec).[1e,7] Subsequently, a variety of hosts including CB[*n*]-type, calixarenes, pillararenes, and organic frameworks have been investigated as reversal agents for neuromuscular blockers.[8]

In 2020, we reported the design and synthesis of sulfated pillar[*n*]arene derivatives dubbed pillar[*n*]MaxQ (**P*n*MQ**, Fig. 1) and showed that **P*n*MQ** display ultratight binding toward hydrophobic (di)cations in sodium phosphate buffered water with high selectivity for tertiary and quaternary ammonium ions including the neuromuscular blocking agents roc and vec.[9] More recently, we showed that **P6MQ** displays good *in vitro* and *in vivo* biocompatibility according to a variety of assays (cytotoxicity, *in vivo* maximum tolerated dose, Ames test, hERG ion channel inhibition), binds tightly to a panel of drugs of abuse, and functions as an *in vivo* sequestrant for methamphetamine and fentanyl.[10] Recently, other groups have reported the synthesis of sulfated versions of other macrocyclic arenes[11] and studied their potential as reversal agents for cisatracurium and hexadimethrine.[12] Herein, we report our study of the interaction of **P6MQ** with a broad panel of neuromuscular blockers and neurotransmitters (Fig. 1) in the more biologically relevant phosphate buffered saline (PBS) and *in vivo* efficacy studies demonstrating that **P6MQ** reverses the effects of roc and vec.

Before proceeding to measure the binding constants for the **P6MQ**·guest complexes, we first set out to glean their geometrical features. Previously, based on analysis of complexation induced changes in ^{1}H NMR chemical shift, we deduced that **P6MQ** binds the hydrophobic regions of guests in its central hydrophobic cavity, whereas pendant cationic groups reside near the anionic sulfate groups.[9,10,13] As an informative example, Fig. 2 shows the ^{1}H NMR spectra recorded for **P6MQ** and roc. The ^{1}H NMR of **P6MQ** (Fig. 2a) shows singlets for H_y and H_z

[a] *College of Pharmacy, Chongqing Medical University, Chongqing 400016, P. R. China. E-mail: xiangjunzhang@cqmu.edu.cn*
[b] *Department of Chemistry and Biochemistry, University of Maryland, College Park, Maryland 20742, USA. E-mail: LIsaacs@umd.edu*

† Electronic supplementary information (ESI) available: Synthetic procedures and characterization, ITC thermograms, ^{1}H NMR spectra of **P6MQ**·guest complexes, and details of *in vivo* studies. See DOI: https://doi.org/10.1039/d4cc00772g

‡ These authors contributed equally.

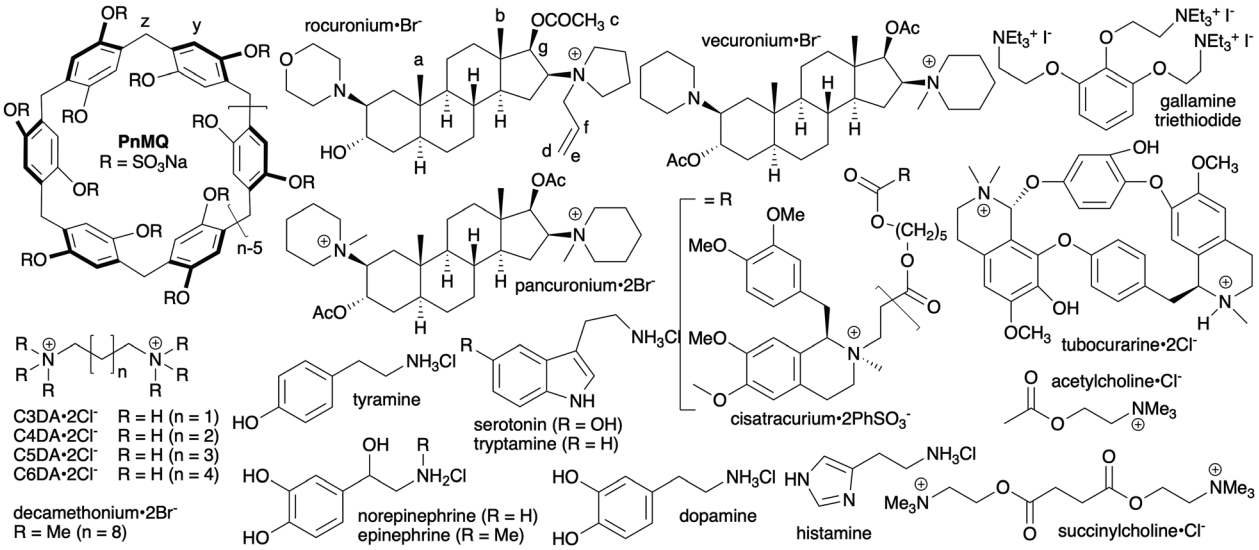

Fig. 1 Chemical structures of **P6MQ**, neuromuscular blockers, neurotransmitters, and competitive guests used in this study.

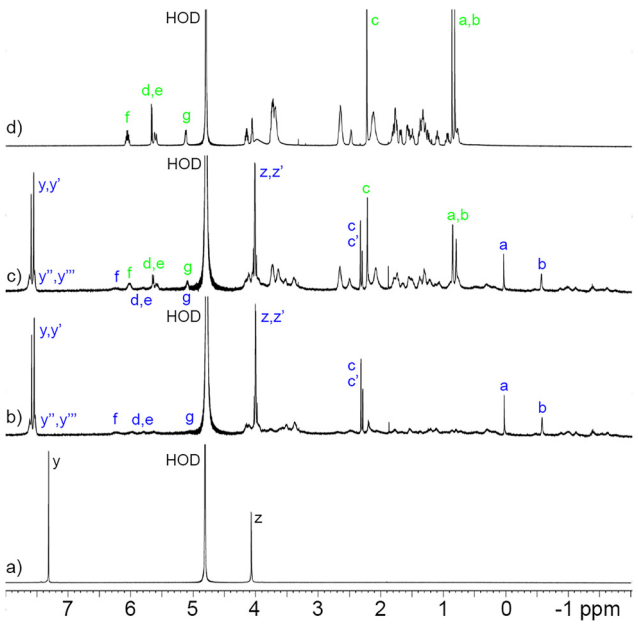

Fig. 2 ^{1}H NMR spectra recorded (600 MHz, D_2O, RT) for: (a) **P6MQ**, (b) an equimolar mixture of **P6MQ** and roc (0.5 mM), (c) a 2 : 1 mixture of roc (1 mM) and **P6MQ** (0.5 mM), and (d) roc. Green labels: rocuronium; blue labels: **P6MQ**·roc.

which is consistent with a racemic mixture of planar chiral forms (p*R* and p*S*)[14] of the depicted D_6-symmetric conformation where the top and bottom sulfated portals are chemically equivalent. Fig. 2d shows the spectrum of roc with key resonances assigned. Upon formation of the **P6MQ**·roc complex (Fig. 2b), we observe that the resonances for the axial steroidal methyl groups (H_a and H_b) are shifted significantly upfield whereas the resonances for the acetoxy CH_3 (H_c) and the pendant allyl group (H_d–H_g) undergo only very small changes in chemical shift. This pattern of chemical shift changes indicates that the hydrophobic steroidal skeleton is bound within the hydrophobic cavity of **P6MQ**, whereas the cationic units reside outside the cavity near the sulfate groups. At a 1 : 2 **P6MQ** : roc ratio (Fig. 2c) we observe separate resonances for **P6MQ**·roc and uncomplexed roc, which indicates guest exchange is slow on the chemical shift timescale, which is commonly observed for tight complexes. Interestingly, for the **P6MQ**·roc complex (Fig. 2b) we observe splitting of H_z into an AB quartet (H_z, $H_{z'}$) due to the binding of the unsymmetrical guest which desymmetrizes the top and bottom portals of **P6MQ** as shown in the MMFF minimized molecular model presented in Fig. 3. Additionally, H_y splits into two sets of two singlets (H_y, $H_{y'}$ and $H_{y''}$, $H_{y'''}$) which we attribute to the presence of two diastereomeric complexes (p*R*-**P6MQ**·roc and p*S*-**P6MQ**·roc). The ^{1}H NMR spectra for the complexes of **P6MQ** with vec, cisatracurium, gallamine triethiodide, decamethonium, succinylcholine, and acetylcholine display related complexation induced changes in chemical shift and are shown in the ESI.†

Next, we turned our attention to the measurement of the **P6MQ**·guest binding constants. Given the tight binding previously observed for **P6MQ** complexes, we decided to use isothermal titration calorimetry (ITC) as our main analytical tool because K_a values in the 10^3–10^7 M^{-1} range can be accurately measured by direct titrations and higher K_a values by competitive ITC

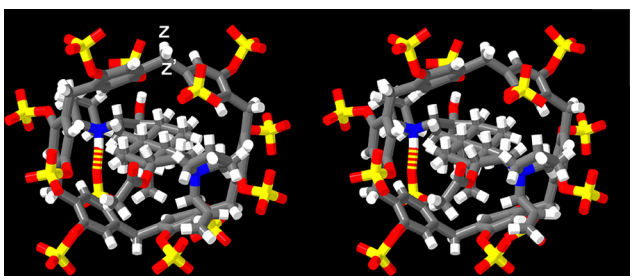

Fig. 3 Cross-eyed stereoview of an MMFF minimized geometry of the **P6MQ**·roc complex. Color code: C, grey; H, white; N, blue; O, red; H-bonds, red-yellow stripped.

Table 1 Binding constants (K_a, M^{-1}), enthalpies (ΔH, kcal mol^{-1}) and c-values measured for **P6MQ**·guest complexes

	K_a (M^{-1})	ΔH (kcal mol^{-1})	c
Rocuronium[d]	$(2.536 \pm 0.004) \times 10^{11}$	-22.03 ± 0.02	90
Vecuronium[d]	$(4.41 \pm 0.01) \times 10^{11}$	-18.60 ± 0.01	150
Decamethonium[d]	$(1.327 \pm 0.001) \times 10^{11}$	-16.77 ± 0.01	49
Gallamine[c]	$(8.11 \pm 0.44) \times 10^{9}$	-13.53 ± 0.04	230
Succinylcholine[c]	$(9.20 \pm 0.13) \times 10^{8}$	-15.23 ± 0.02	26
Pancuronium[c]	$(2.18 \pm 0.11) \times 10^{8}$	-11.60 ± 0.04	61
Tubocurarine[a]	$(5.03 \pm 0.10) \times 10^{5}$	-12.27 ± 0.05	50
Cisatracurium[a]	$(3.89 \pm 0.39) \times 10^{5}$	-15.17 ± 0.26	39
C3DA[a]	$(5.95 \pm 0.32) \times 10^{4}$	-4.79 ± 0.06	15
C4DA[a]	$(3.53 \pm 0.05) \times 10^{6}$	-6.04 ± 0.01	350
C5DA[b]	$(3.43 \pm 0.65) \times 10^{7}$	-10.27 ± 0.15	55
C6DA[b]	$(2.73 \pm 0.03) \times 10^{8}$	-9.48 ± 0.03	45
Acetylcholine[a]	$(2.55 \pm 0.15) \times 10^{6}$	-9.29 ± 0.06	130
Histamine[a]	$(3.77 \pm 0.20) \times 10^{5}$	-15.47 ± 0.14	38
Tyramine[a]	$(3.19 \pm 0.05) \times 10^{5}$	-9.60 ± 0.03	5
Dopamine[a]	$(8.02 \pm 0.76) \times 10^{4}$	-9.40 ± 0.26	8
Tryptamine[a]	$(5.35 \pm 0.11) \times 10^{4}$	-9.40 ± 0.07	5
Epinephrine[a]	$(4.39 \pm 0.17) \times 10^{4}$	-9.44 ± 0.14	5
Norepinephrine[a]	$(9.06 \pm 0.14) \times 10^{3}$	-8.64 ± 0.05	5
Serotonin[a]	$(9.04 \pm 0.26) \times 10^{3}$	-9.88 ± 0.11	5

Conditions: PBS, 298.15 K. [a] Measured by direct ITC titration. [b] Measured by competitive ITC titration using a mixture of **P6MQ** and C3Da in the cell. [c] Measured by competitive ITC titration using a mixture of **P6MQ** and C4DA in the cell. [d] Measured by competitive ITC titration using a mixture of **P6MQ** and C6DA in the cell.

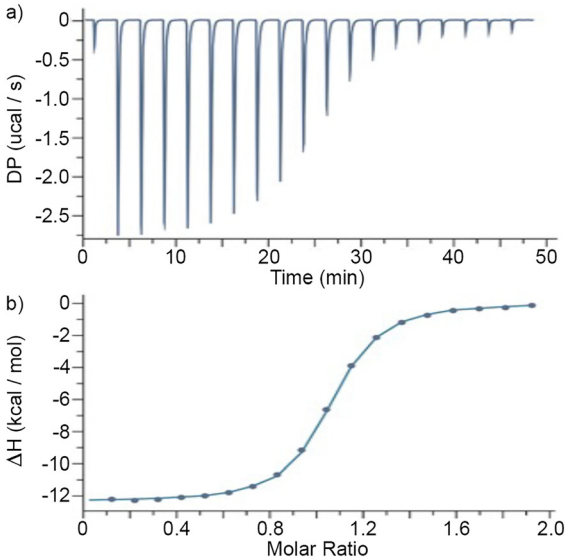

Fig. 4 (a) Plot of DP *versus* time from the competitive titration of a mixture of **P6MQ** (100 μM) and C6DA (1.00 mM) in the cell with roc (1.00 mM) from the syringe (PBS buffer, pH 7.4, 298 K). (b) Plot of ΔH *versus* molar ratio. The solid line represents the best non-linear fit of the data to a competition binding model ($K_a = (2.536 \pm 0.004) \times 10^{11}$ M^{-1}, $\Delta H = -22.03 \pm 0.02$ kcal mol^{-1}, $-T\Delta S = 6.44 \pm 0.02$ kcal mol^{-1}).

titrations.[15] The measurements were performed in the more competitive and biologically relevant PBS (pH 7.4) buffer. For the weaker complexes between **P6MQ** and all eight neurotransmitters and two NMBAs (cisatracurium and tubocurarine) we performed direct titrations in triplicate (ESI†) and report the average K_a, ΔH and Wiseman c-values in Table 1. For the tighter complexes with the NMBAs where appropriate Wiseman c-values could not be achieved in direct titrations,[15b] we performed competitive ITC titrations. For this purpose, we employed C3DA–C6DA, which bind with increasing K_a and different ΔH values as the chain length increases, thereby allowing the selection of an appropriate competitor for a given NMBA. The K_a and ΔH values for the **P6MQ**·competitor complexes were determined by direct titrations (Table 1) and used as known inputs to analyze the competitive ITC titrations. Fig. 4a shows a plot of DP *versus* time recorded when a solution of **P6MQ** (100 μM) and C6DA (1.00 mM) in the cell was titrated with a solution of roc (1.00 mM) from the syringe. Integration of the peaks in Fig. 4a allowed the construction of Fig. 4b which shows a plot of ΔH *versus* molar ratio. Fig. 4b was fitted to a competitive binding model to extract the K_a (2.53×10^{11} M^{-1}) and ΔH (-22.03 kcal mol^{-1}) values for the **P6MQ**·roc complex (Table 1). Please note that Fig. 4b plateaus at ≈ -12.5 kcal mol^{-1} which represents the difference in ΔH values between the competing **P6MQ**·C6DA and **P6MQ**·roc complexes. The remaining tight complexes were measured analogously (Table 1). As expected, the stoichiometry of the **P6MQ**·guest complexes given in Table 1 are 1 : 1 as determined by the ITC n-value. The cavity of **P6MQ** is not large enough to comfortably form ternary complexes with even the smallest guests. The K_a values range from 10^3–10^{11} M^{-1} with large and negative ΔH values consistent with complexation driven by the non-classical hydrophobic effect.[16] **P6MQ** binds the steroidal NMBAs roc and vec with picomolar affinity which is 10 000-fold stronger than sugammadex which is used clinically.[1e] Importantly, **P6MQ** displays $\geq 10^5$-fold selectivity for roc and vec relative to acetylcholine which is also present in the neuromuscular junction. **P6MQ** displays even higher levels of discrimination against the other neurotransmitters which suggests that **P6MQ** has great potential as an *in vivo* reversal agent for NMBAs.

Given the exceptionally tight **P6MQ**·roc and **P6MQ**·vec complexes and the discrimination against neurotransmitters, we decided to perform *in vivo* efficacy studies. All studies were approved by the Institutional Animal Care and Use Committee at Chongqing Medical University (Approval number: IACUC-CQMU-2022-0025). A total of 12 male and 12 female Sprague-Dawley rats (220–320 g) were anesthetized with isoflurane and equipped with intravenous lines along with subcutaneous electrodes to stimulate the femoral nerve supramaximally and the response of the quadriceps femoris was monitored using the Veryark-TOF (Guangxi VERYARK Technology Co., Ltd, China). The femoral nerve was continuously stimulated for 10 minutes before recalibration of the Veryark-TOF and administration of rocuronium (3.5 mg kg^{-1}, 5.74 μmol kg^{-1}) or vecuronium (0.7 mg kg^{-1}, 1.1 μmol kg^{-1}). These doses of roc and vec were previously determined as twice the ED90 which is the dose required to decrease the twitch height by 90%.[17] The rats were continuously ventilated and then the reversal agent (saline, **P6MQ** (5.74 μmol kg^{-1} for roc; 1.1 μmol kg^{-1} for vec), or sugammadex (5.74 μmol kg^{-1} for roc; 1.1 μmol kg^{-1} for vec)) were administered 30 seconds later. Please note that equimolar quantities of NMBA and reversal agent were administered. The time required for the train-of-four ratio to return to 90% of

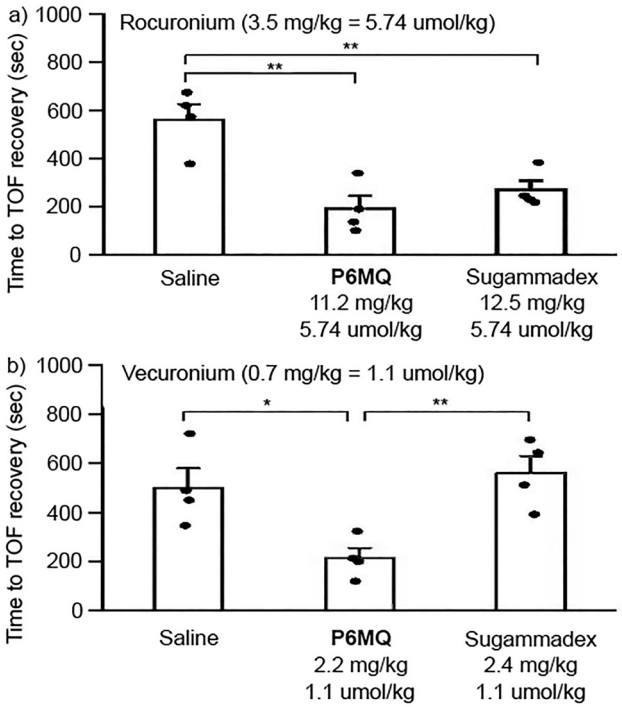

Fig. 5 Results of the *in vivo* efficacy studies conducted using Sprague-Dawley rats. Rats (n = 4 per group) were anesthetized with isoflurane and treated with a neuromuscular blocker: (a) rocuronium (3.5 mg kg^{-1}) or (b) vecuronium (0.7 mg kg^{-1})) and then treated with saline, **P6MQ**, or sugammadex. Error bars represent means and standard deviation, *p < 0.05; **p < 0.01 (unpaired two-tailed t-test).

baseline T1 were determined and are plotted as a function of treatment group in Fig. 5. Fig. 5a shows that both **P6MQ** and sugammadex display comparable efficacy (p = 0.278) at accelerating the recovery of the train-of-four (TOF ratio to 90% of baseline when roc is used as NMBA relative to saline as placebo). In contrast, when vec (1.1 μmol kg^{-1}) is used as NMBA (Fig. 5b), an equimolar dose of **P6MQ** (1.1 μmol kg^{-1}) is effective at accelerating the recovery of the TOF ratio to 90% whereas an equimolar dose of sugammadex (1.1 μmol kg^{-1}) is not effective.

In summary, we have established that **P6MQ** forms tight complexes with several NMBAs (roc, vec, decamethonium, gallamine triethiodide, succinylcholine, and pancuronium) *in vitro* and functions as a highly effective *in vivo* reversal agent for roc and vec. This work, when combined with our earlier work on the reversal of drugs of abuse using **P6MQ**[10] and related work on sulfated macrocyclic arenes,[12] further establishes the high potential of **P6MQ** in a variety of biomedical applications.

L. I., E. A. B.-B., and A. P. D. thank the University of Maryland for financial support. X. Z. and W. Z. thank the Chongqing Medical University for financial support.

Conflicts of interest

L. I. holds equity in Reversal Therapeutics (National Harbor, Maryland, USA) and Clear Scientific (Cambridge, Massachusetts, USA). The other authors have no conflicts to declare.

Notes and references

1 (*a*) D. J. Cram, *Angew. Chem., Int. Ed. Engl.*, 1988, **27**, 1009–1020; (*b*) J.-M. Lehn, *Angew. Chem., Int. Ed. Engl.*, 1988, **27**, 89–112; (*c*) J. F. Stoddart, *Angew. Chem., Int. Ed.*, 2017, **56**, 11094–11125; (*d*) K. Harris, D. Fujita and M. Fujita, *Chem. Commun.*, 2013, **49**, 6703–6712; (*e*) A. Bom, M. Bradley, K. Cameron, J. K. Clark, J. Van Egmond, H. Feilden, E. J. MacLean, A. W. Muir, R. Palin, D. C. Rees and M.-Q. Zhang, *Angew. Chem., Int. Ed.*, 2002, **41**, 265–270.

2 (*a*) M. Rekharsky and Y. Inoue, *Chem. Rev.*, 1998, **98**, 1875–1917; (*b*) F. Diederich, *Angew. Chem., Int. Ed. Engl.*, 1988, **27**, 362–386; (*c*) J. H. Jordan and B. C. Gibb, *Chem. Soc. Rev.*, 2015, **44**, 547–585; (*d*) K. I. Assaf and W. M. Nau, *Chem. Soc. Rev.*, 2015, **44**, 394–418; (*e*) T. Ogoshi, T.-A. Yamagishi and Y. Nakamoto, *Chem. Rev.*, 2016, **116**, 7937–8002; (*f*) H. Yin, X. Zhang, J. Wei, S. Lu, D. Bardelang and R. Wang, *Theranostics*, 2021, **11**, 1513–1526; (*g*) V. Böhmer, *Angew. Chem., Int. Ed. Engl.*, 1995, **34**, 713–745; (*h*) T. J. Finnegan, V. W. L. Gunawardana and J. D. Badjic, *Chem. – Eur. J.*, 2021, **27**, 13280–13305.

3 R. A. Rajewski and V. J. Stella, *J. Pharm. Sci.*, 1996, **85** 1142–1169.

4 (*a*) F. M. Roland and B. D. Smith, *Supramol. Chem. Water*, 2019, pp. 501–524, DOI: 10.1002/9783527814923.ch13; (*b*) J. Yeon, S. J. Kim, H. Jung, H. Namkoong, J. Tang, B. W. Hwang, K. Oh, K. Kim, Y. C. Sung and S. K. Hahn, *Adv. Healthcare Mater.*, 2015, **4**, 237–244.

5 Y.-C. Pan, J.-H. Tian and D.-S. Guo, *Acc. Chem. Res.*, 2023, **56**, 3626–3639.

6 (*a*) C.-L. Deng, S. L. Murkli and L. D. Isaacs, *Chem. Soc. Rev.*, 2020, **49**, 7516–7532; (*b*) S. Ganapati and L. Isaacs, *Isr. J. Chem.*, 2018, **58**, 250–263.

7 J. M. Adam, D. J. Bennett, A. Bom, J. K. Clark, H. Feilden, E. J. Hutchinson, R. Palin, A. Prosser, D. C. Rees, G. M. Rosair, D. Stevenson, G. J. Tarver and M.-Q. Zhang, *J. Med. Chem.*, 2002, **45**, 1806–1816.

8 (*a*) X. Zhang, Q. Cheng, L. Li, L. Shangguan, C. Li, S. Li, F. Huang, J. Zhang and R. Wang, *Theranostics*, 2019, **9**, 3107–3121; (*b*) U. Hoffmann, M. Grosse-Sundrup, K. Eikermann-Haerter, S. Zaremba, C. Ayata, B. Zhang, D. Ma, L. Isaacs and M. Eikermann, *Anesthesiology*, 2013, **119**, 317–325; (*c*) Y. Chai, L. Chen, Y. Zhang, L. Zhao, Z. Meng, J. Chen, C. Li and Q. Meng, *Chin. Chem. Lett.*, 2022, **33**, 3003–3006; (*d*) H.-K. Liu, F. Lin, S.-B. Yu, Y. Wu, S. Lu, Y.-Y. Liu, Q.-Y. Qi, J. Cao, W. Zhou, X. Li, H. Wang, D.-W. Zhang, Z.-T. Li and D. Ma, *J. Med. Chem.*, 2022, **65**, 16893–16901; (*e*) A. J. Selinger, N. A. Cavallin, A. Yanai, I. Birol and F. Hof, *Angew. Chem., Int. Ed.*, 2022, **61**, e202113235; (*f*) Y. Wu, Y.-Y. Liu, H.-K. Liu, S.-B. Yu, F. Lin, W. Zhou, H. Wang, D.-W. Zhang, Z.-T. Li and D. Ma, *Chem. Sci.*, 2022, **13**, 9243–9248.

9 W. Xue, P. Y. Zavalij and L. Isaacs, *Angew. Chem., Int. Ed.*, 2020, **59**, 13313–13319.

10 A. T. Brockett, W. Xue, D. King, C.-L. Deng, C. Zhai, M. Shuster, S. Rastogi, V. Briken, M. R. Roesch and L. Isaacs, *Chemistry*, 2023, **9**, 881–900.

11 X.-N. Han, Y. Han and C.-F. Chen, *Chem. Soc. Rev.*, 2023, **52**, 3265–3298.

12 (*a*) Y. Zhao, L. Chen, C. Junyi, J. Li, Q. Meng, A. C.-H. Sue and C. Li, *Chem. Commun.*, 2023, **59**, 5858–5861; (*b*) R. Wang, W.-B. Li, J.-Y. Deng, H. Han, F.-Y. Chen, D.-Y. Li, L.-B. Jing, Z. Song, R. Fu, D.-S. Guo and K. Cai, *Angew. Chem., Int. Ed.*, 2023, e202317402, DOI: 10.1002/anie.202317402.

13 (*a*) C.-L. Deng, M. Cheng, P. Y. Zavalij and L. Isaacs, *New J. Chem.*, 2022, **46**, 995–1002; (*b*) D. King, C.-L. Deng and L. Isaacs, *Tetrahedron*, 2023, **145**, 133607.

14 J.-F. Chen, J.-D. Ding and T.-B. Wei, *Chem. Commun.*, 2021, **57**, 9029–9039.

15 (*a*) T. Wiseman, S. Williston, J. F. Brandts and L.-N. Lin, *Anal. Biochem.*, 1989, **179**, 131–137; (*b*) J. Broecker, C. Vargas and S. Keller, *Anal. Biochem.*, 2011, **418**, 307–309; (*c*) A. Velazquez-Campoy and E. Freire, *Nat. Protocols*, 2006, **1**, 186–191.

16 E. Persch, O. Dumele and F. Diederich, *Angew. Chem., Int. Ed.*, 2015, **54**, 3290–3327.

17 M. Eikermann, S. Zaremba, A. Malhotra, A. S. Jordan, C. Rosow and N. L. Chamberlin, *Br. J. Anaesth.*, 2008, **101**, 344–349.